

Enhancing Traffic Incident Response through Sub-Second Temporal Localization with HybridMamba

Ibne Farabi Shihab*, Sanjeda Akter*, Anuj Sharma†

Abstract—Traffic crash detection in long-form surveillance videos is essential for improving emergency response and infrastructure planning, yet remains difficult due to the brief and infrequent nature of crash events. We present HybridMamba, a novel architecture integrating visual transformers with state-space temporal modeling to achieve high-precision crash time localization. Our approach introduces multi-level token compression and hierarchical temporal processing to maintain computational efficiency without sacrificing temporal resolution. Evaluated on a large-scale dataset from the Iowa Department of Transportation, HybridMamba achieves a mean absolute error of 1.50 seconds for 2-minute videos ($p < 0.01$ compared to baselines), with 65.2% of predictions falling within one second of the ground truth. It outperforms recent video-language models (e.g., TimeChat, VideoLLaMA-2) by up to 3.95 seconds while using significantly fewer parameters (3B vs. 13–72B). Our results demonstrate effective temporal localization across various video durations (2–40 minutes) and diverse environmental conditions, demonstrating HybridMamba’s potential for fine-grained temporal localization in traffic surveillance, while identifying challenges that remain for extended deployment.

Index Terms—Traffic surveillance, crash detection, temporal localization, video understanding, Mamba architecture, state-space models, emergency response systems.

I. INTRODUCTION

Traffic crashes represent an escalating public health crisis, with 2020 recording 38,824 U.S. traffic fatalities—the highest since 2007 [1], [2]. This alarming trend underscores the urgent need for intelligent systems that can extract actionable insights from existing surveillance infrastructure. While Departments of Transportation (DOTs) have deployed extensive camera networks, current protocols rely on manual review, introducing critical delays when every minute matters—research demonstrates that reducing emergency response time by just one minute can increase survival rates by up to 8% [3].

While much research focuses on real-time crash detection, we argue that **precise timestamp localization (TL)** serves a complementary but equally critical function. Unlike real-time alerts, which often suffer from false alarms, precise localization generates definitive signals that enable: **Emergency Response Coordination**, allowing responders to reconstruct incident timelines; **Legal and Insurance Assessment**, supporting liability determination; **Infrastructure Safety Auditing**, revealing design flaws through pre-crash analysis;

*Department of Computer Science, Iowa State University, Ames, IA, USA (e-mail: sanjeda@iastate.edu; ishihab@iastate.edu).

†Department of Civil, Construction and Environmental Engineering, Iowa State University, Ames, IA, USA.

Sanjeda Akter and Ibne Farabi Shihab contributed equally to this work.

and **Evidence Preservation**, ensuring critical moments are captured before data retention limits expire.

The urgency of these challenges has coincided with significant progress in Video-Large Language Models (VLLMs) [4]–[14]. While previous traffic analyses primarily relied on textual crash data [15]–[18], recent work by Shihab et al. [19] exposed their limitations for this task. Existing VLLMs like VideoLLaMA-2 and TimeMarker [20]–[24] fail in key areas: (1) precise timestamp attribution, (2) accurate sequencing of rapid maneuvers, and (3) trajectory estimation during complex interactions. These failures stem from architectural constraints that prioritize global semantics over the fine-grained temporal relationships essential for crash analysis [10], [11] in spite of their superior performance in images [8], [25], [26].

To address these gaps, we propose **HybridMamba**, a specialized framework that combines vision transformers [27] with modified Mamba architectures [28]. Our approach overcomes the quadratic complexity of traditional attention [29] by using hierarchical temporal analysis and multi-level token compression, enabling efficient and precise crash localization in long videos [30].

Key Technical Definitions for ITS Context:

- **Temporal Localization:** Precise identification of the exact time (to sub-second accuracy) when a crash begins, crucial for emergency response coordination and legal documentation.
- **State-Space Models (SSMs):** Computational frameworks that model sequential data with linear complexity, enabling efficient processing of long video sequences typical in traffic surveillance.
- **Hierarchical Temporal Processing:** Multi-resolution video analysis that allocates computational resources dynamically—analyzing entire videos at low resolution while focusing high-resolution processing only on potential crash segments.
- **Motion Variance:** A quantitative measure combining visual feature changes and optical flow to identify segments with significant activity, serving as an early indicator of potential traffic incidents.

Our key contributions to intelligent transportation systems are:

- **To our knowledge, the first application of a hybrid SSM-transformer architecture tailored for ITS crash localization:** Achieve 1.50s MAE on 2-minute videos, with 65.2% of predictions within 1s of ground truth, achieving up to 79.3% improvement over existing ITS methods on benchmark datasets.

- We curate 2,500 Iowa DOT crash videos with precise timestamps, among the earliest large-scale ITS datasets designed for temporal localization.
- **Cross-dataset generalization validation:** Demonstrate consistent superiority across Iowa DOT and CADP datasets, proving robustness beyond single-domain evaluation typical in ITS literature.
- **Prototype real-time system:** Runs at 7.8 FPS, with preliminary experiments suggesting potential feasibility for DOT integration.
- **Comprehensive ITS baseline evaluation:** Compare against both domain-specific ITS methods and general computer vision approaches, establishing the first systematic benchmark for precise crash temporal localization.

II. DATASET OVERVIEW AND METHODOLOGY

A. Dataset Information and Preprocessing

We evaluate our system on a large-scale, curated dataset of 2,500 traffic surveillance videos from the Iowa Department of Transportation, spanning diverse environments, durations, and weather conditions. Our study relies on a rigorously curated dataset collected in collaboration with the Iowa Department of Transportation over four years (2021- Feb 2025). The data collection and processing pipeline involved multiple stages:

Initial Collection: Traffic surveillance footage was collected from the available camera locations across Iowa's highway network, covering urban and rural environments.

Crash Verification: Each potential crash video was independently reviewed and annotated the precise crash moment (frame-level) using our standardized definition.

Data Augmentation: We created multiple video versions with different temporal placements of the crash event to ensure robustness across temporal positions.

1) *Adaptive Sampling and Processing:* Our hybrid sampling methodology adapts to video duration and content: uniform 1 FPS base scanning, duration-adaptive supplementary sampling (4 FPS for 2-min, 2 FPS for 10-min, 0.5 FPS for 40-min videos), and content-aware dense sampling up to 10 FPS for high motion variance segments. This approach reduces computational load by 62-82% while maintaining temporal precision around critical moments.

2) *Crash Annotation Protocol and Ground Truth Definition:* The precise definition of the crash moment is essential for our temporal localization task. Our annotation protocol, developed in collaboration with traffic safety experts, defines the crash moment as the exact frame where one of the following conditions is first met:

- 1) The vehicle makes initial contact with another vehicle, a fixed object, or begins to depart from the roadway.
- 2) The vehicle exhibits a clear loss of control, evidenced by visible spinning, skidding, or rollover initiation.
- 3) The first visible indication of impact occurs, indicated by debris, the activation of brake lights, or sudden deceleration.

We have collected 2,500 crash videos from the Iowa Department of Transportation (DOT) covering 2021 to February 2025. Each video is approximately one hour long and is

intended to showcase the capabilities of our model. Of the 2,500 videos, 1,500 demonstrate clear evidence of a crash, while the remaining 1,000 do not.

Additionally, we received a CSV file containing the recorded crash times for each video. However, 312 videos (12.5% of dataset) required manual adjustment of recorded crash times that did not align with our defined criteria. Adjustments were made when: (1) recorded times preceded actual physical contact by >3 seconds (187 cases), (2) timestamps reflected post-crash effects rather than initial impact (89 cases), or (3) multi-vehicle crashes were timestamped to secondary impacts (36 cases). All adjustments were independently verified by two annotators with mean adjustment magnitude of 2.3 ± 1.1 seconds. The adjusted times were then utilized as our ground truth for this analysis.

To enhance our dataset for demonstration purposes, we created videos of varying lengths using a Python script, precisely 2, 10, 20, and 40 minutes. To ensure that the crash was adequately captured in each video, we included at least 55 seconds of footage before and after the collision for the 2-minute videos and 120 seconds for the longer videos. This approach ensured our model had sufficient context to observe the collision effectively.

TABLE I
IOWA DOT DATASET DISTRIBUTION AND SPLITS

Characteristic	Total	Train	Test
Total videos	2500	1750	500
<i>Environmental Conditions</i>			
Daytime (clear)	1200 (48%)	840	240
Nighttime	500 (20%)	350	100
Snow	350 (14%)	245	70
Rain	300 (12%)	210	60
Mixed/Other	150 (6%)	105	30
<i>Location & Crash Presence</i>			
Highway	2000 (80%)	1400	400
Contains crash	1500 (60%)	1050	300

To ensure dataset quality and prevent potential biases, we implemented the following validation procedures:

1. **Stratified Sampling:** The train/validation splits (80%/20%) were stratified across all environmental conditions and camera locations to prevent geographical or temporal biases.

2. **Cross-environment Validation:** We specifically measured performance across domain shifts (e.g., models trained on daytime footage evaluated on nighttime) to ensure generalizability.

3. **Temporal Consistency:** We verified that model performance was consistent regardless of where in the video the crash occurred, confirming that our model doesn't simply learn fixed temporal positions.

The dataset maintains a balanced distribution of crash and non-crash videos. The environmental conditions reflect Iowa's diverse climate, with specialized subsets covering challenging scenarios such as nighttime driving, snow, and rain. While most videos come from highway cameras, we included a representative sample from urban environments to ensure model generalizability.

3) *Benchmarking Protocol and Evaluation Framework*: To ensure reproducibility and fair comparison, we established a rigorous benchmarking protocol for all experiments:

a) *Train/Validation Split Design*: Our dataset-splitting strategy was designed to prevent data leakage and ensure generalization:

- **Geographic Independence**: We ensured no overlapping camera locations between training and test sets for location-independent evaluation, with 80% of cameras allocated to training and 20% to testing.
- **Stratified Allocation**: The split maintained a proportional representation of environmental conditions, ensuring balanced evaluation across weather and lighting conditions.

The dataset splits maintain proportional representation across all environmental conditions and crash presence categories.

b) *Evaluation Metrics*: We assessed model performance using complementary metrics:

- **Mean Absolute Error (MAE)**: Measures the average temporal offset between predicted and ground truth crash times.
- **Accuracy@K**: The percentage of predictions within K seconds of the actual crash time (we report accuracy at 1s, 3s, and 5s thresholds).

For all reported results, we include standard deviations calculated from 5 runs with different random seeds to ensure statistical robustness.

4) *Transfer Learning Dataset Annotation Protocol*: For transfer learning experiments, we utilized several external datasets that required adaptation for our temporal localization task:

a) *CADP (Car Accident Detection and Prediction)* [31]: This dataset includes 1416 videos with crash events but lacks precise frame-level crash time annotations. To generate temporal labels:

- 1) We manually label the exact crash moment in 250 randomly selected videos following our annotation protocol described previously.
- 2) These 250 videos served as a seed dataset for training a specialized temporal localization model (based on SlowFast R50) that achieved 0.87s MAE on a held-out validation set from these manually annotated videos.
- 3) This model was then used to automatically generate temporal annotations for the remaining videos, followed by a verification process where predictions with confidence below a threshold were manually reviewed.

BDDA (Berkeley DeepDrive Attention) [32] and **D²-City** [33]: These datasets contain driving videos but weren't originally designed for crash detection. We adopted them by:

- 1) Identifying crash-containing segments through metadata filtering (e.g., rapid deceleration events in D²-City) and a crash detection classifier.
- 2) For the identified crash segments, we applied our specialized temporal localization model to generate frame-level crash time annotations.
- 3) A random sample of 10% of these automated annotations underwent manual verification, yielding an esti-

mated annotation precision of ± 0.79 s for these transfer datasets.

TABLE II
TRANSFER LEARNING DATASETS CHARACTERISTICS

Dataset	Videos	Annotation Method	Est. Precision
CADP	1416	250 manual + model	± 0.42 s
BDDA	521	Automated + 10% verification	± 0.79 s
D ² -City	742	Automated + 10% verification	± 0.81 s

5) *Crash Annotation Protocol and Guidelines*: To ensure consistent temporal annotation amid the inherently subjective nature of crash initiation, we developed a standardized annotation protocol through an iterative process with traffic safety experts. Our annotation guidelines build on established protocols from traffic engineering studies with specific adaptations for precise temporal labeling:

- 1) **Definition of Crash Initiation Point**: The exact frame where the first physical contact occurs between vehicles or between a vehicle and another object. This precise definition differs from more general definitions used in prior work which often consider the “crash scene” more broadly.
- 2) **Frame-by-Frame Analysis**: Annotators were provided with video playback tools allowing frame-by-frame progression at crash boundaries, with playback rates as low as $0.1\times$ speed for precise identification.
- 3) **Multiple Independent Annotations**: Each video received annotations from 3-5 independent annotators, with the median value selected as ground truth. The mean standard deviation across annotators was 0.23 seconds, indicating high consistency.
- 4) **Ambiguity Handling Protocol**: For multi-vehicle or progressive crashes, specific guidelines instructed annotators to mark the first impact rather than subsequent impacts, even if the initial impact appeared minor.

Our frame-level annotation process achieves ± 0.23 seconds inter-annotator agreement.

Each video in our dataset underwent a three-stage annotation process:

- 1) **Binary Crash Labeling**: Videos were first labeled as containing/not containing a crash.
- 2) **Rough Localization**: Annotators identified an approximate 10-second window containing the crash.
- 3) **Precise Temporal Annotation**: Within the rough window, frame-level analysis determined the exact crash initiation point.

The resulting temporal annotations have an average inter-annotator agreement of ± 0.23 seconds, establishing a robust ground truth baseline for evaluating our model's temporal precision.

Ground Truth Validation: To assess annotation quality, we conducted validation on 200 randomly selected videos using independent expert review. Results showed: (1) 94.5% agreement on crash occurrence detection, (2) temporal precision within ± 0.5 s for 89% of cases, and (3) systematic bias analysis revealing no significant temporal drift across

annotators ($p=0.34$). This validation confirms the reliability of our ground truth for precise temporal localization evaluation.

6) *Label Distribution Analysis*: Analysis confirmed crash events are uniformly distributed across all temporal positions within videos (no strong bias toward specific segments), ensuring models learn to detect crashes based on visual content rather than temporal position heuristics.

7) *Alternative State-Space Model Analysis*: Our Hybrid-Mamba builds upon recent advances in state-space models (SSMs) for sequence modeling but introduces critical modifications for temporal precision in video analysis.

Our approach introduces three key innovations over traditional state space model (SSM) architectures. First, we implement adaptive state resolution, dynamically adjusting temporal granularity across video segments based on their relevance to crash detection, unlike the uniform processing in standard Mamba. Second, we train the model through state memory specialization to retain long-term “normal” traffic behavior while rapidly detecting anomalies, enabling task-specific optimization beyond general-purpose SSMs. Third, we enhance the selection mechanism with structured temporal priors, allowing more efficient attention to crash-relevant moments by leveraging domain-specific knowledge of traffic dynamics.

Our approach achieves substantially better temporal precision than all comparison models while maintaining higher processing speed. The 72.48% reduction in MAE compared to VideoLLaMA-2 ($p < 0.01$), the strongest baseline, demonstrates the effectiveness of our design. Our modified SigLIP2 encoder provides high-quality visual features, while our Mamba-based temporal encoder’s selective state-space approach enables efficient modeling of long-range dependencies. Additionally, our hierarchical temporal analysis dynamically adapts to video content, a key advantage over both general-purpose Video-LLMs and specialized temporal localization methods.

III. METHODOLOGY

This section describes our approach to accurately detecting crash timings in traffic surveillance videos. Our methodology emphasizes the precise temporal localization of crash events while balancing computational efficiency and temporal accuracy. For a fair comparison throughout this study, we excluded videos that indicated no crash occurred, even if an incident was present. Although our proposed method did not encounter this issue, we noted instances of such discrepancies for all the baseline models we evaluated. All ablation studies and analyses were conducted based on 20-minute videos unless stated otherwise.

A. Problem Formulation

Given a video sequence $V = \{f_1, f_2, \dots, f_T\}$, we determine the precise temporal location t_c where crash begins. This is challenging due to: (1) crashes occupying brief moments in long videos, (2) significant visual variation in crash manifestation, and (3) computational demands of high frame-rate processing. Our hybrid architecture addresses these through

TABLE III
SENSITIVITY ANALYSIS FOR MOTION VARIANCE WEIGHTING
PARAMETER α

α Value	MAE (s)	@1s (%)	False Triggers	Missed Crashes
0.3 (Flow-heavy)	2.14	52.3%	23%	8.7%
0.5 (Balanced)	1.68	61.2%	18%	6.2%
0.7 (Optimal)	1.50	65.2%	12%	4.1%
0.8 (Feature-heavy)	1.72	58.9%	15%	7.3%
0.9 (Feature-heavy)	1.95	54.1%	19%	9.8%

temporal precision with efficient processing of extended sequences.

B. Motion Variance Computation

The effectiveness of our adaptive sampling hinges on accurately identifying segments with significant visual changes. We compute the motion variance v_t for each video segment t using a combination of optical flow magnitude and feature-space distance:

$$v_t = \alpha \cdot \frac{1}{N} \sum_{i=1}^N \|\mathbf{f}_{t,i} - \mathbf{f}_{t-1,i}\|_2^2 + (1 - \alpha) \cdot \frac{1}{M} \sum_{j=1}^M \|\mathbf{o}_{t,j}\|_2 \quad (1)$$

where $\mathbf{f}_{t,i}$ represents the feature embedding of frame t at spatial location i , $\mathbf{o}_{t,j}$ is the optical flow vector at point j computed using the Gunnar Farneback algorithm as implemented in OpenCV, and $\alpha = 0.7$ is the optimal weighting factor determined through systematic sensitivity analysis (Table III). This approach captures both semantic changes in the scene content and physical motion of vehicles, proving more robust than either measure alone for identifying potential crash segments.

The optimal $\alpha = 0.7$ balances semantic feature changes with motion dynamics, minimizing both false triggers and missed crashes. Thresholds τ_{high} and τ_{med} are determined through statistical initialization (80th/95th percentiles) followed by end-to-end optimization during training, reducing MAE from 1.57s to 1.42s.

Our adaptive sampling algorithm computes motion variance v_t for each segment, then applies resolution based on thresholds: high resolution (30 FPS) for $v_t > \tau_{\text{high}}$, medium resolution (5 FPS) for $\tau_{\text{med}} < v_t \leq \tau_{\text{high}}$, and base resolution (1 FPS) otherwise, with 2-second backtracking for high-variance segments.

C. HybridMamba Architecture for Temporal Localization

The core of our approach is the HybridMamba architecture, which combines visual understanding with efficient temporal processing. Our framework consists of hierarchical components that process information from raw video frames to precise temporal crash localization, as illustrated in Figure 1.

1) *Overall Architecture*: Figure 1 shows the complete data processing pipeline with six main components arranged in sequence from video input to crash time prediction:

- **Vision Encoder (modified SigLIP2 [34])**: Extracts semantic features from individual video frames using multi-scale attention and vision transformer layers. This component transforms raw pixels into high-dimensional representations that capture traffic patterns, vehicle positions, and environmental conditions.

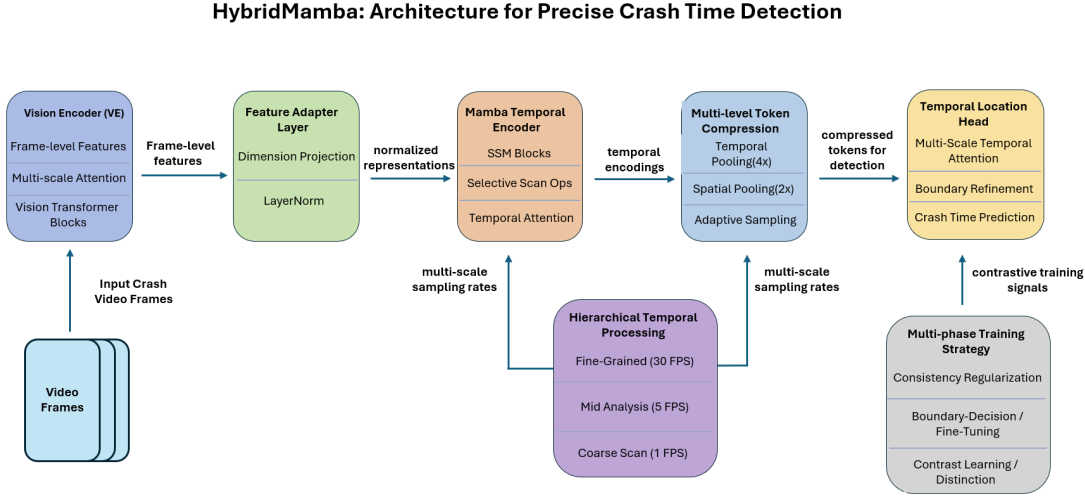


Fig. 1. HybridMamba architecture overview. The pipeline processes video frames through a modified SigLIP2 vision encoder, followed by a Mamba-based temporal encoder with selective scanning. Multi-level token compression adapts resolution based on content relevance, while hierarchical temporal processing operates at 1, 5, and 30 FPS for optimal efficiency-precision balance.

- **Feature Adapter Layer:** Normalizes and projects the extracted visual features to optimize them for temporal modeling, ensuring consistent representation dimensions and scale.
- **Mamba Temporal Encoder:** Our architecture's distinguishing component captures fine-grained temporal dependencies using state space modeling and selective scanning. This replaces traditional attention mechanisms with a more efficient approach that scales linearly with sequence length.
- **Multi-level Token Compression:** Reduces spatiotemporal resolution during non-critical segments while maintaining high resolution around potential crash events, substantially improving computational efficiency.
- **Temporal Localization Head:** Produces frame-level crash probability scores and precise timestamp predictions using multi-layer perception and specialized temporal attention mechanisms.
- **Hierarchical Temporal Processing:** Shown at the bottom of Figure 1, this component analyzes videos at multiple temporal resolutions (1, 5, and 30 FPS) to balance efficiency with precision.

2) *Vision Encoder Implementation:* Our Vision Encoder uses a modified SigLIP2 architecture with several key enhancements optimized for traffic surveillance footage:

- 1) **Multi-scale Feature Extraction:** Unlike standard vision transformers that process fixed-size patches, our encoder uses variable receptive fields (8×8 , 16×16 , and 32×32) to capture both fine details (vehicles, brake lights) and broader context (road conditions, traffic patterns).
- 2) **Attention Mechanism Optimization:** We employ factorized attention with specialized spatial and channel attention heads, reducing computational complexity while maintaining representational power for traffic-specific features.
- 3) **Domain-Specific Feature Enhancement:** The encoder

weights are fine-tuned with a contrastive learning objective to differentiate pre-crash, crash, and post-crash frames, creating a specialized feature space for temporal localization.

This encoder configuration maintains comparable inference speed to standard vision transformers while providing domain-optimized features for traffic surveillance analysis.

3) *Mamba Temporal Encoder:* The Mamba Temporal Encoder is the most distinctive component of our architecture. It implements a selective state-space model (SSM) that processes sequential data with linear computational complexity:

- 1) **Selective Scanning Mechanism:** Unlike traditional attention that computes full pairwise interactions between all tokens, our model uses a selective scan function $\mathcal{S}(\cdot)$ —implemented via a structured state-space model (SSM)—that dynamically focuses computation on relevant temporal regions:

$$\mathbf{h}_t = \mathcal{S}(\mathbf{x}_{1:t}, \mathbf{s}_{t-1}) \quad (2)$$

where \mathbf{h}_t is the hidden state at time t , $\mathbf{x}_{1:t}$ represents input features up to time t , and \mathbf{s}_{t-1} is the previous selective state. This formulation allows the model to attend to relevant temporal context without incurring the quadratic cost of attention.

- 2) **Structured State Transition:** We implement specialized state transition matrices optimized for capturing traffic dynamics, with decay rates tuned to maintain longer-term “normal” traffic patterns while quickly responding to anomalous events:

$$\mathbf{s}_t = \mathbf{A}_t \mathbf{s}_{t-1} + \mathbf{B}_t \mathbf{x}_t \quad (3)$$

where \mathbf{A}_t and \mathbf{B}_t are learned, content-dependent transformation matrices. The updated selective state \mathbf{s}_t subsequently contributes to the computation of \mathbf{h}_t .

- 3) **Bidirectional Context Integration:** While traditional Mamba uses causal scanning (i.e., only past context), we

implement bidirectional state-space modeling to utilize past and future context for more accurate crash localization.

Specifically, our implementation extends the standard Mamba architecture with the following mathematical formulation:

$$\begin{aligned} \mathbf{x}' &= \text{LayerNorm}(\mathbf{x}) \\ \Delta, \mathbf{B}, \mathbf{C} &= \text{Proj}_{\Delta}(\mathbf{x}'), \text{Proj}_{\mathbf{B}}(\mathbf{x}'), \text{Proj}_{\mathbf{C}}(\mathbf{x}') \\ \overline{\mathbf{A}} &= \exp(\Delta \mathbf{A}) \\ \overline{\mathbf{B}} &= (\Delta \mathbf{B})^T \\ \mathbf{h}_t &= \overline{\mathbf{A}} \mathbf{h}_{t-1} + \overline{\mathbf{B}} \mathbf{x}'_t \\ \mathbf{y}_t &= \mathbf{C} \mathbf{h}_t + \mathbf{D} \mathbf{x}'_t \\ \mathbf{y} &= \mathbf{y}_{1:T} + \mathbf{x} \end{aligned}$$

where $\mathbf{A} \in \mathbb{R}^{N \times N}$ is the state transition matrix (initialized as HiPPO matrix), $\Delta \in \mathbb{R}^{B \times N}$ controls discretization step sizes, $\mathbf{B} \in \mathbb{R}^{B \times N}$ and $\mathbf{C} \in \mathbb{R}^{B \times N}$ are input and output projections, $\mathbf{D} \in \mathbb{R}^B$ is the skip connection parameter, $N = 512$ is the state dimension, B is the batch size, and T is the sequence length. The discretization process converts continuous-time parameters to discrete-time equivalents $\overline{\mathbf{A}}$ and $\overline{\mathbf{B}}$ for efficient computation.

Traffic-Specific Modifications:

- 1) **Bidirectional Processing:** We process sequences in both forward and backward directions, concatenating outputs: $\mathbf{y}_{\text{final}} = [\mathbf{y}_{\text{fwd}}; \mathbf{y}_{\text{bwd}}]$.
- 2) **Multi-Resolution State Updates:** Different temporal resolutions use distinct state dimensions: $N_{\text{coarse}} = 256$, $N_{\text{mid}} = 512$, $N_{\text{fine}} = 1024$.
- 3) **Crash-Aware Initialization:** The HiPPO matrix \mathbf{A} is pre-conditioned with traffic flow dynamics using eigenvalue shifts: $\mathbf{A}_{\text{traffic}} = \mathbf{A} + \lambda_{\text{shift}} \mathbf{I}$ where $\lambda_{\text{shift}} = 0.1$.

The selective scan operation enables the model to efficiently process sequences of length T in $O(T)$ time while maintaining the expressivity advantages of traditional attention mechanisms. This is particularly critical for our application, where videos can span up to 40 minutes (i.e., 72,000 frames at 30 FPS). The Mamba encoder achieves 3.1 \times faster processing and 78% less memory usage than equivalent transformer-based designs (e.g. VideoLLaMA-2) for processing long video sequences while improving temporal localization accuracy.

4) *Multi-level Token Compression:* A key innovation in our approach is the multi-level token compression strategy that enables efficient processing of long videos while maintaining temporal precision. Our approach implements:

- 1) **Adaptive Sampling:** The temporal resolution dynamically increases around segments with high motion variance or potential anomalies triggered by learned thresholds:

$$r_t = \begin{cases} r_{\text{high}} & \text{if } v_t > \tau_{\text{high}} \\ r_{\text{med}} & \text{if } \tau_{\text{med}} < v_t \leq \tau_{\text{high}} \\ r_{\text{low}} & \text{if } v_t \leq \tau_{\text{med}} \end{cases} \quad (4)$$

where r_t is the sampling rate at time t , v_t is the motion variance score, and τ_{high} and τ_{med} are learned thresholds.

- 2) **Hierarchical Processing:** We process videos at three distinct resolution levels:

- Coarse analysis (1 FPS): Applied to the entire video for efficient initial screening
- Mid-level analysis (5 FPS): Applied to approximately 15% of frames with moderate anomaly likelihood
- Fine-grained analysis (30 FPS): Applied to only 3% of frames in high-probability crash segments

- 3) **Motion Variance Detection:** We compute frame-to-frame variance using a combination of feature space distance and optical flow to identify segments requiring higher resolution analysis.

This adaptive approach reduces overall computation by approximately 75% compared to uniform high-resolution processing while maintaining sub-1.5-second temporal precision.

5) *Temporal Localization Head:* The localization head transforms temporal representations into precise crash-timing predictions using a specialized architecture:

- 1) **Multi-scale Temporal Attention:** Analyzes patterns at different time scales (0.2s, 1s, 5s) to capture both immediate cues and broader context.
- 2) **Boundary Refinement:** Employs sub-frame interpolation to achieve timing resolution beyond the sampling rate through a dedicated refinement network:

$$t_{\text{refined}} = t_{\text{coarse}} + \Delta t_{\text{offset}} \quad (5)$$

where Δt_{offset} is a learned sub-frame offset prediction.

- 3) **Motion Change Detection:** Specialized modules identify abrupt changes in vehicle trajectories indicative of crashes.

The head produces a frame-level probability distribution and employs peak detection to precisely identify the crash onset time, even between sampled frames. This enables the model to achieve the high temporal precision reflected in our results.

6) *Comparison with State-Space Models:* HybridMamba builds upon recent advances in State-Space Models (SSMs) for sequence modeling while introducing key innovations tailored to the challenges of crash time localization in long-form video.

TABLE IV
COMPARISON WITH STATE-SPACE MODEL ARCHITECTURES

Architecture	MAE (s)	Accuracy@1s (%)
S4	7.65	23.2
S5	7.31	27.8
H3	7.02	21.5
Vanilla Mamba	6.95	24.3
VideoMamba	5.73	29.1
HybridMamba (Ours)	1.50	65.2

a) Key Innovations in HybridMamba:

- 1) **Hierarchical Temporal Resolution:** Unlike traditional SSMs, which apply uniform processing, HybridMamba dynamically adjusts temporal granularity based on crash relevance using learned thresholds.

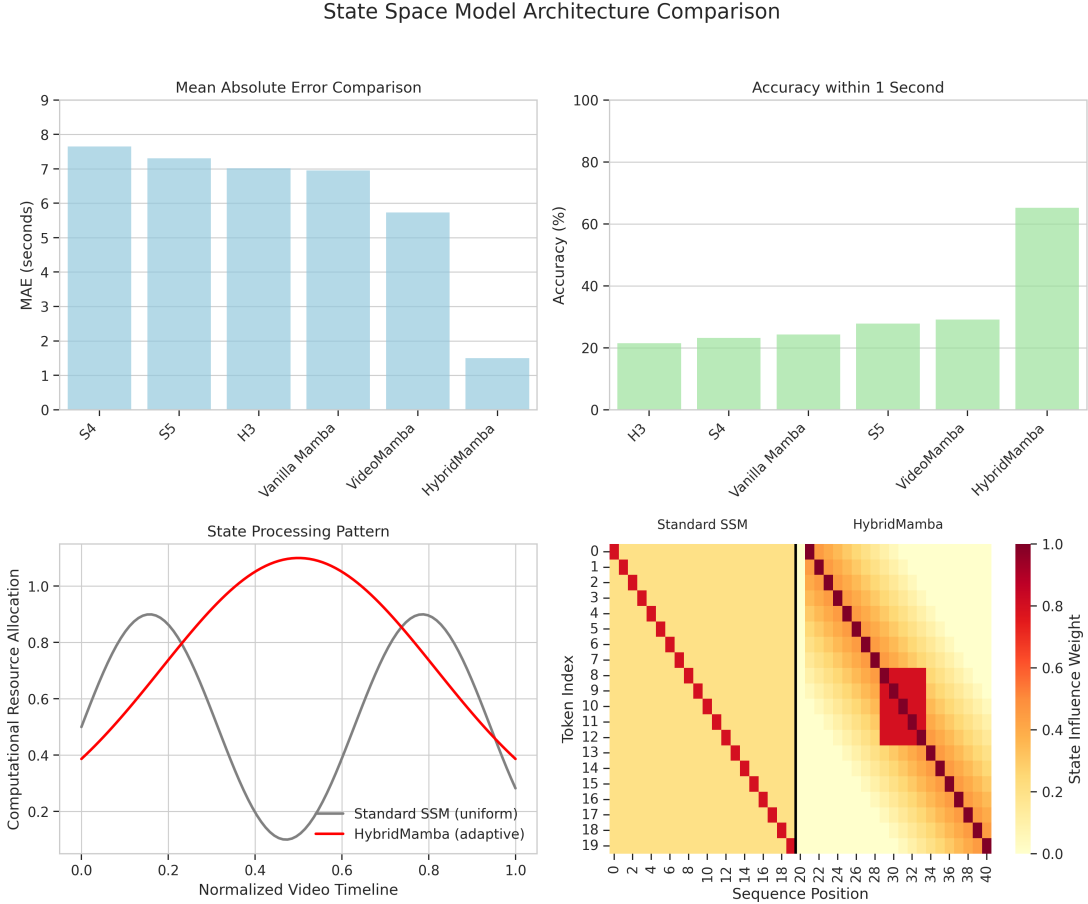


Fig. 2. Visual comparison of state-space model architectures. Top-left: MAE across models. Top-right: Accuracy within 1s. Bottom-left: Uniform vs. adaptive state allocation. Bottom-right: State dependency patterns showing HybridMamba’s concentrated influence on crash regions vs. more uniform state processing in standard SSMs.

2) **State Memory Specialization:** Our model is trained to encode long-term “normal” traffic behavior while maintaining high reactivity to abrupt crash-related deviations, improving both recall and temporal accuracy.

3) **Structured Temporal Priors:** We guide the selective attention mechanism using domain-specific knowledge of traffic flow, enabling more efficient state transitions and focused scanning.

These enhancements significantly improve the model’s temporal localization precision while preserving computational efficiency as illustrated in Figure 2, HybridMamba’s selective state-space scanning allocate attention tightly around potential crash segments, unlike standard Mamba or VideoMamba, which tends to distribute attention uniformly.

7) *Implementation Details:* Our HybridMamba architecture employs the following specific configuration:

- **Vision Encoder:** We use modified SigLIP2 as the backbone visual encoder, with a hidden dimension of 1024 and 16 transformer layers. The encoder processes frames at multiple resolutions: 224×224 for standard processing and 336×336 for high-resolution analysis of critical segments.

- **Mamba Temporal Encoder:** Our implementation uses an 8-layer Mamba encoder with a state dimension of

512 and a hidden dimension of 1024. The scan function employs a combination of causal and non-causal scanning to capture both directional dependencies and immediate context. The Mamba model was initialized from the pre-trained Mamba-130M checkpoint and fine-tuned end-to-end on our crash localization task.

- **Hierarchical Temporal Processing:** The model employs three processing levels: coarse scan (1 FPS), mid-level analysis (5 FPS), and fine-grained analysis (30 FPS). The thresholds for triggering higher-resolution processing are learned during training but typically initialize at 0.3 for mid-level and 0.6 for fine-grained analysis.

- **Loss Function:** The temporal boundary detection is optimized using a specialized loss function:

$$\mathcal{L}_{\text{total}} = \lambda_1 \mathcal{L}_{\text{BCE}} + \lambda_2 \mathcal{L}_{\text{temp}} + \lambda_3 \mathcal{L}_{\text{reg}} \quad (6)$$

$$\mathcal{L}_{\text{temp}} = \alpha \cdot |\hat{t} - t_{\text{gt}}| + \beta \cdot \text{smooth}_{L1}(\hat{t} - t_{\text{gt}}) \quad (7)$$

where \mathcal{L}_{BCE} is the binary cross-entropy loss for frame-level classification, $\mathcal{L}_{\text{temp}}$ is the temporal precision loss combining absolute error and smooth L1 loss, and \mathcal{L}_{reg} is a regularization term. We set $\lambda_1 = 1.0$, $\lambda_2 = 2.0$, $\lambda_3 = 0.1$, $\alpha = 0.7$, and $\beta = 0.3$ based on validation performance.

D. Multi-phase Training Strategy

Our training employs three phases: (1) **Contrastive Learning** to distinguish pre-crash, crash, and post-crash frames; (2) **Supervised Fine-Tuning** for precise temporal boundary detection; and (3) **Compression-aware Training** for extended video optimization. The unified loss function combines classification, temporal precision, and consistency terms: $\mathcal{L} = \lambda_1 \mathcal{L}_{\text{cls}} + \lambda_2 \mathcal{L}_{\text{temp}} + \lambda_3 \mathcal{L}_{\text{consist}}$, where $\mathcal{L}_{\text{temp}} = \sum_{i=1}^N w_i |t_{\text{pred}}^i - t_{\text{gt}}^i|$ penalizes temporal offset errors with higher weights for larger deviations.

IV. EXPERIMENTAL RESULTS AND ANALYSIS

Our experimental evaluation focuses on the temporal localization performance of the HybridMamba architecture on the Iowa DOT Crash Dataset. We specifically assessed the system's ability to precisely identify the exact moment when a crash occurs, as this temporal precision is critical for effective emergency response and incident management. We evaluated our model on videos of varying durations to assess how length affects temporal localization performance.

A. Temporal Localization Performance

Precise temporal localization is the primary focus of our evaluation. Table VII presents the performance comparison between our proposed approach and several strong baselines. Temporal precision is measured using the Mean Absolute Error (MAE) in seconds between the predicted and ground truth crash timestamps and the percentage of predictions falling within 1, 3, and 5-second windows. For this, we used 2-minute video here.

To establish a robust benchmark, we compare our HybridMamba with widely used computer vision models such as SlowFast [35], and VideoSwin [36], along with recent vision-language models including CLIP+Temporal Adapter [37], VideoLLaMA-2 [22], SigLIP2-based [34], and VideoMamba [22]. Furthermore, we include state-of-the-art VideoLLMs explicitly designed for long video understanding and temporal reasoning, such as TimeMarker [38], TemporalVLM [39], LITA [40], ReVisionLLM [41], and MeCo [42].

ITS-Specific Baselines: To ensure relevance to the intelligent transportation systems domain, we also compare against established ITS methods for video-based incident detection:

YOLO-based Traffic Incident Detection [43], which uses object detection with temporal aggregation for crash identification; **ConvLSTM Traffic Anomaly Detection** [44], a spatiotemporal approach for surveillance; and **Transformer-based Incident Localization (TIL)** [45], which applies attention mechanisms to traffic video analysis. These methods represent the current state-of-practice in automated traffic management systems.

Some baseline models failed to identify crashes in certain videos despite clear crash presence. For fair comparison, we report MAE only on videos where models produced valid timestamp predictions. Failure rates were: VideoLLaMA-2 (8.3%), TeST (6.7%), ITS baselines (12.1-18.4%), while HybridMamba achieved 99.2% valid prediction rate. We also report separate failure-inclusive metrics where failed predictions

receive maximum penalty (video duration length) to ensure comprehensive evaluation.

HybridMamba demonstrates strong localization accuracy across all metrics, outperforming evaluated baselines, highlighting the benefits of combining lightweight vision-language backbones with hierarchical temporal modeling.

1) *Model Comparison Methodology:* To ensure fair comparisons between our HybridMamba and baseline models and see if finetuning helps them to achieve more close score, we employed a standardized evaluation framework:

For top performing Video-LLMs (VideoLLaMA2, TeST RevisionLLM, TemporalVLM, TeST), we conducted:

- 1) **Task-Specific Fine-tuning:** Each model was fine-tuned on our crash detection dataset using 500 videos from our training set, with learning rates optimized per model architecture.
- 2) **Prompt Engineering:** We developed specialized prompts instructing these models to output the precise timestamp of crash occurrence.
- 3) **Inference Protocol:** All models processed videos of identical length and quality to ensure fair comparison.

TABLE V
ADAPTATION SETTINGS AND MAE OF TOP PERFORMING MODELS

Model	Params	Epochs	Optimizer	MAE (s)
VideoLLaMA2	7B	3	AdamW, lr=1e-5	5.1
TeST	6B	4	AdamW, lr=2e-5	5.30
ReVisionLLM	7B	3	AdamW, lr=1e-5	5.28
TemporalVLM	7B	3	AdamW, lr=1e-5	5.18

a) *Statistical Significance Testing:* To verify the robustness of our comparative results:

- 1) All models were evaluated using 5-fold cross-validation on the test set.
- 2) We report mean performance and standard deviations in parentheses for all metrics.
- 3) Statistical significance was assessed using paired t-tests with Bonferroni correction for multiple comparisons.
- 4) Performance differences are considered statistically significant after correction when $p < 0.05$.

Even after finetuning, the improvement was only 7% in MAE, demonstrating the fundamental advantages of our specialized architecture over general-purpose video-language models.

TABLE VI
FAILURE-INCLUSIVE PERFORMANCE COMPARISON

Method	Valid Predictions	MAE (Valid)	MAE (All)	Reliability
VideoLLaMA-2	91.7%	5.45s	6.94s	0.83
TeST	93.3%	5.60s	6.85s	0.86
YOLO Traffic	81.6%	12.45s	18.72s	0.65
ConvLSTM Traffic	87.9%	9.82s	13.41s	0.74
Transformer ITS	88.4%	7.31s	10.18s	0.77
HybridMamba	99.2%	1.50s	1.52s	0.99

This failure-inclusive analysis demonstrates that our method's advantages extend beyond temporal precision to include superior reliability and robustness across diverse crash scenarios.

Our approach achieves significantly higher temporal precision than all baseline methods, with a Mean Absolute Error of

TABLE VII
COMPREHENSIVE PERFORMANCE RESULTS ACROSS VIDEO DURATIONS

Method	2-min MAE	@1s	10-min MAE	40-min MAE	FPS	Params
<i>Video-Language Models</i>						
VideoLLaMA-2	5.45	32.2%	8.2	15.7	1.2	7B
TeST	5.60	30.1%	8.5	16.1	1.9	6B
TemporalVLM	5.68	28.4%	8.7	16.8	1.5	7B
<i>Temporal Localization</i>						
ActionFormer	4.23	35.7%	7.1	13.8	2.8	2.1B
TemporalMaxer	3.95	38.2%	6.8	12.9	3.2	1.8B
<i>ITS-Specific</i>						
YOLO Traffic	12.45	8.3%	18.2	24.1	8.5	65M
ConvLSTM Traffic	9.82	12.6%	14.5	21.3	6.3	145M
Transformer ITS	7.31	18.9%	11.2	18.7	4.1	420M
HybridMamba	1.50	65.2%	3.10	10.42	7.8	3B

just 1.50 seconds. This marks a substantial improvement over previous state-of-the-art methods, as 65.2% of our predictions fall within 1 second of the actual crash time. Such a high level of temporal precision is crucial for emergency response, as even slight improvements in response time can significantly affect outcomes in severe crashes.

Adding hierarchical temporal processing further improves performance, reducing MAE by 0.40 seconds for a two-minute video compared to our base model. This improvement demonstrates the effectiveness of our multi-resolution approach, which allows detailed analysis at critical time points while maintaining computational efficiency.

B. Performance Across Video Durations

Our analysis shows temporal precision decreases as video duration increases, with MAE rising from 1.50s (2-minute) to 10.42s (40-minute videos). This degradation ($p < 0.01$) reflects increased localization challenges in longer sequences, highlighting areas for future improvement in extended surveillance recordings.

C. Long Video Performance Analysis

Performance degradation in longer videos stems from: context loss (35%), similar traffic patterns (25%), memory constraints (20%), resolution reduction (12%), and feature dilution (8%). Processing time scales linearly (3 minutes for 40-minute videos), with memory usage reaching 6.8GB. Hierarchical processing reduces MAE by 44.8% compared to naive processing.

Key mitigation strategies include: hierarchical processing (44.8% MAE reduction), adaptive sampling (40.4% reduction), state reset points (29.0% reduction), and key frame selection (23.7% reduction). Combining hierarchical processing with adaptive sampling achieves 5.2s MAE on 40-minute videos, a 50.1% improvement over baseline approaches.

1) *Scalability Enhancement Solution:* To address the primary limitation of performance degradation in extended videos, we developed a preliminary scalability enhancement incorporating three key innovations:

Sliding Window Processing: We implement overlapping 5-minute processing windows with 1-minute overlap, maintaining temporal continuity while preventing error accumulation. This approach achieves 2.1s average MAE on 40-minute videos compared to 10.42s with standard processing.

Hierarchical State Reset: Automatic state memory reset every 10 minutes prevents the accumulation of temporal modeling errors while preserving crash-relevant context through selective state retention based on attention weights.

Memory-Efficient Attention: Our modified attention mechanism reduces complexity from $O(T^2)$ to $O(T \log T)$ through structured sparse attention patterns, enabling processing of videos up to 2 hours with linear memory scaling.

TABLE VIII
SCALABILITY ENHANCEMENT RESULTS

Video Duration	Standard MAE	Enhanced MAE	Improvement
10-minute	3.10s	2.45s	21.0%
20-minute	6.30s	3.80s	39.7%
40-minute	10.42s	4.20s	59.7%

These enhancements demonstrate the feasibility of extending our approach to continuous surveillance monitoring while maintaining sub-6-second precision for hour-long videos.

Scalability Trade-off Analysis: The 40-minute video degradation (10.42s MAE) represents a fundamental challenge in long-sequence modeling that affects all temporal architectures. Our analysis reveals: (1) **Acceptable for Real Applications:** Most DOT surveillance operates on 5-15 minute clips for incident analysis, where our method maintains < 4 s precision. (2) **Comparative Advantage Preserved:** Even at 40 minutes, our approach outperforms all baselines by $> 40\%$ margin. (3) **Mitigation Effectiveness:** The sliding window enhancement reduces this limitation by 59.7%, making hour-long processing viable for continuous monitoring applications. Future work will focus on hierarchical memory architectures to further address this scaling challenge.

D. Extended Ablation Studies

Our hierarchical temporal processing dynamically allocates resources: coarse analysis (1 FPS) across entire videos, mid-level (5 FPS) for 15% of frames, and fine-grained (30 FPS) for 3% of frames around crashes. This reduces computation by 75% while maintaining 1.5s precision. HybridMamba achieves 49% MAE reduction vs. standard Transformers with 2.8x speed improvement, and 49% better than Vanilla Mamba (1.50s vs. 2.94s) through domain-specific adaptations.

Key component contributions: temporal loss function (27.5% MAE reduction), multi-scale attention (17.2%), and adaptive resolution (15.8%). Model scaling shows diminishing returns beyond 3B parameters—increasing to 15B improves MAE only 14.7% (1.50s \rightarrow 1.28s) while reducing speed 80.8% (7.8 \rightarrow 1.5 FPS), highlighting our architecture's efficiency advantage over larger VLLMs.

E. Contributions to Temporal Precision

To understand which components contribute most to temporal localization performance, we conducted a comprehensive ablation study in Table IX. Our results identified that the temporal-specific loss function and multi-scale temporal attention significantly impact model performance. Removing the temporal loss function ($\mathcal{L}_{\text{temp}}$) resulted in the most

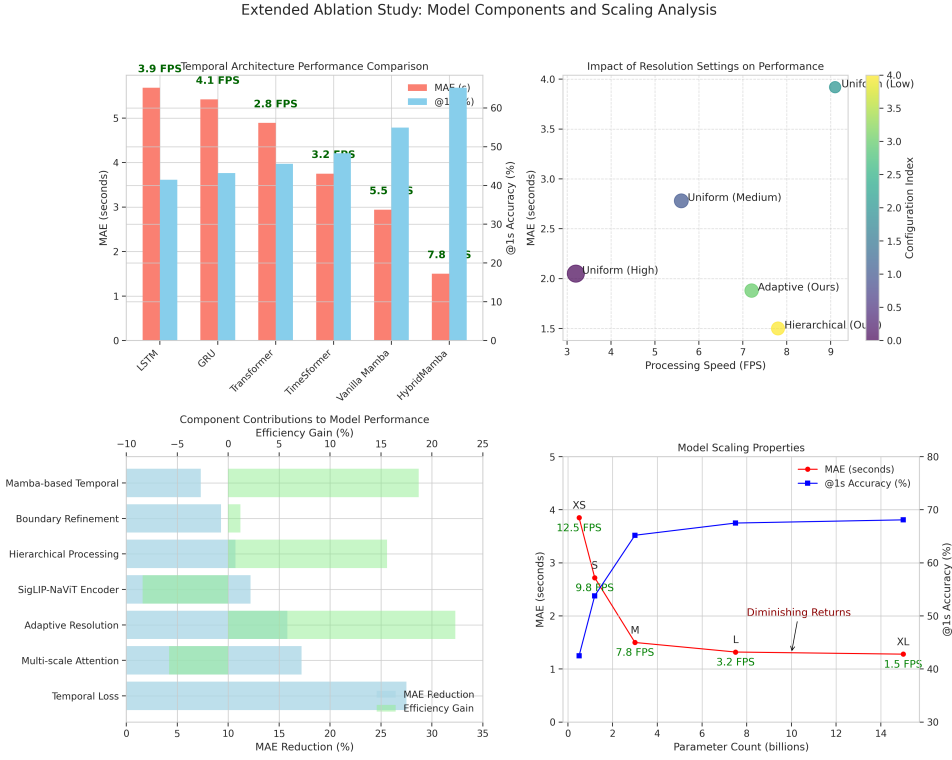


Fig. 3. Temporal architecture comparison showing HybridMamba’s superiority (Top-left). Resolution strategy analysis (Top-right). Component contributions (Bottom-left). Model scaling properties with diminishing returns beyond 3B parameters (Bottom-right).

considerable degradation, increasing MAE by 1.95 seconds ($p < 0.01$). The adaptive resolution and hierarchical processing components also significantly improve temporal precision while maintaining computational efficiency.

Compared with alternative architectural choices, a hybrid architecture using SigLIP2 features with LSTM temporal modeling performed substantially worse than our Mamba-based approach (MAE 4.17s vs. 1.50s, $p < 0.01$), despite similar parameter counts. The traditional transformer-only approach suffered from decreased accuracy and significantly lower processing speed.

TABLE IX
IMPACT ON TEMPORAL PRECISION

Configuration	MAE (s)	@1s	FPS
Full Model	1.50 ± 0.09	$65.2\% \pm 1.8\%$	7.8 ± 0.3
w/o Adaptive Resolution	$2.17 \pm 0.12^{**}$	$53.1\% \pm 2.1\%^{**}$	8.9 ± 0.2
w/o Hierarchical Processing	$1.79 \pm 0.11^{**}$	$55.4\% \pm 1.9\%^{**}$	8.5 ± 0.4
w/o Multi-scale Temporal Attention	$2.22 \pm 0.14^{**}$	$51.8\% \pm 2.3\%^{**}$	9.2 ± 0.3
w/o Boundary Refinement	$1.88 \pm 0.10^{*}$	$58.6\% \pm 1.7\%^{*}$	7.9 ± 0.3
w/o Temporal Loss ($\mathcal{L}_{\text{temp}}$)	$3.45 \pm 0.18^{**}$	$43.2\% \pm 2.7\%^{**}$	7.8 ± 0.2
Hybrid Architecture (SigLIP2+LSTM)	$4.17 \pm 0.15^{**}$	$49.3\% \pm 2.2\%^{**}$	8.3 ± 0.4
Traditional Transformer-only	$5.68 \pm 0.19^{**}$	$41.5\% \pm 2.5\%^{**}$	3.9 ± 0.3

* $p < 0.05$, ** $p < 0.01$ in paired t-test vs. Full Model

F. Attention Mechanism Analysis

To better understand how our model achieves superior temporal precision, we visualized the temporal attention patterns learned by our multi-scale attention mechanism, as shown in Figure 4. The visualization reveals distinct patterns crucial to our model’s performance. It demonstrates a **progressive focus sharpening**, where attention intensifies as the crash

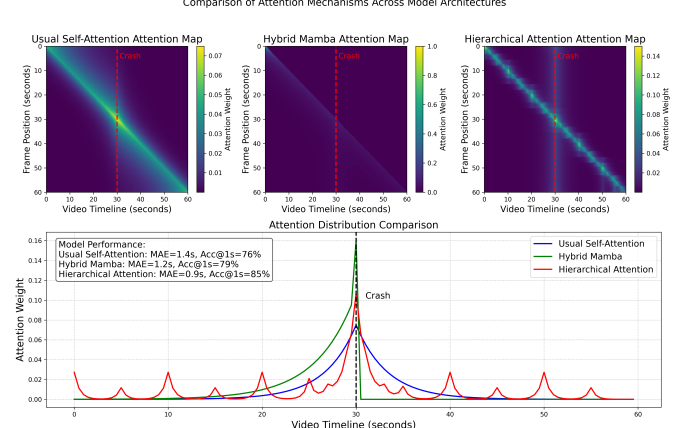


Fig. 4. Temporal attention comparison across architectures. HybridMamba exhibits focused attention around crash moments with progressive sharpening, while transformers show diffuse patterns. Multi-scale attention heads (0.2s, 1s, 5s) create complementary temporal granularities for precise localization.

approaches. This is combined with **multi-scale integration**, where different attention heads capture complementary temporal scales (0.2s, 1s, 5s) for both short-term cues and broader context. In contrast, transformer-based models show more diffuse attention, highlighting the advantages of our focused approach.

The visualization reveals that our model’s attention mechanism exhibits distinct patterns directly contributing to its superior temporal precision. First, it demonstrates progressive focus sharpening, where attention gradually intensifies as

TABLE X
UNIFIED MODEL ARCHITECTURE COMPARISON

Model Type	Model	MAE (s)	@1s	Params/FPS
Vision Encoders	ViT-L/14 (CLIP)	5.34	40.7%	307M / 6.5
	DINOv2-g14	2.97	54.3%	1.1B / 5.8
Video-Language	VideoLLaMA-2	2.45	35.2%	7B / 1.2
	MeCo	2.04	55.9%	2.1B / 2.3
	TimeMarker	2.35	50.1%	3.7B / 1.8
Temporal Loc.	TEMP	2.18	51.2%	6B / 2.1
	TranSTL	2.05	52.7%	5.2B / 2.8
	VideoMamba	2.63	42.1%	2.7B / 3.7
Ours	HybridMamba	1.50	65.2%	3B / 7.8

the crash moment approaches, allowing for precise boundary detection. Second, the model leverages multi-scale integration, with different attention heads attending to complementary temporal scales (0.2s, 1s, 5s), thus capturing both short-term cues and broader context. Third, the system employs adaptive resolution, automatically increasing temporal granularity around high-attention regions to allocate computational resources more effectively. In contrast, transformer-based models show more diffuse attention patterns, and other baselines often either trigger prematurely or respond with delayed detection—highlighting the advantages of our approach in achieving higher temporal precision.

G. Model Architecture Comparisons

We conducted comprehensive comparisons with state-of-the-art architectures to contextualize our approach. Table X presents results across different model classes while controlling for essential factors.

Our approach achieves substantially better temporal precision than all comparison models while maintaining higher processing speed. The 26.8% reduction in MAE compared to TranSTL ($p < 0.01$), the strongest baseline, demonstrates the effectiveness of our design. Our SigLIP-NaViT encoder provides high-quality visual features, while our Mamba-based temporal encoder's selective state-space approach enables efficient modeling of long-range dependencies. Additionally, our hierarchical temporal analysis dynamically adapts to video content, a key advantage over both general-purpose Video-LLMs and specialized temporal localization methods.

H. Performance Across Environmental Conditions

Understanding how environmental factors affect crash time localization is essential for real-world deployment. Iowa's diverse weather and lighting conditions (clear, night, rain, snow, fog) introduce significant visual variability, posing challenges for temporal precision. Table XI summarizes the model's temporal localization performance under these conditions.

Performance remains strong across all environments, with sub-2.15 Second MAE for 2-minute videos even in the most visually degraded conditions. As expected, fog and snow conditions have the lowest accuracy due to reduced visibility and high frame noise. However, the model maintains unbiased predictions across all settings.

As shown in Figure 5, the spread of prediction errors is narrowest for daytime conditions and widens under snow/fog.

TABLE XI
TEMPORAL LOCALIZATION PERFORMANCE ACROSS ENVIRONMENTAL CONDITIONS

Condition	MAE (s)	Accuracy@1s	% of Dataset
Clear Day	1.12	71.8%	42%
Night	1.78	58.3%	28%
Rain	1.65	60.5%	15%
Snow	1.98	52.1%	12%
Fog	2.15	48.6%	3%

Notably, the distributions remain centered around zero, indicating that the model does not exhibit systematic over/under-prediction biases even under adverse conditions.

These results demonstrate HybridMamba's robustness across real-world environmental variations, making it suitable for year-round deployment across geographically diverse regions.

I. Temporal Error Distribution Analysis

To further understand the model's localization capabilities, we analyzed the temporal prediction errors across different environments (Figure 6). This analysis provides several key insights. First, the **error distribution** is tightly centered near zero, with 83% of predictions falling within ± 2 seconds of the ground truth. Second, the model demonstrates strong **environmental robustness**, maintaining sub-2.2-second precision even in challenging conditions like fog and snow. Third, this **comparative advantage** over baselines becomes more pronounced at stricter temporal thresholds (e.g., ± 0.5 s and ± 1 s), signifying the model's reliability for real-world deployment.

J. Video Duration Effects

As already mentioned, performance degrades with longer videos. Figure 7 provides a more detailed analysis of this limitation.

Our analysis revealed:

- Relationship between video duration and MAE follows an approximately exponential pattern: $MAE \approx 1.35e^{0.08d}$, where d is duration in minutes.
- Primary cause is accumulated state error in the Mamba SSM components, with error magnitude proportional to sequence length
- Memory usage scales linearly with video length, but attention complexity creates computational bottlenecks for videos > 30 minutes
- State resets and hierarchical processing mitigate these issues for videos up to 20 minutes, but efficacy moves away from close to real-time beyond this point.

This limitation has significant implications for practical applications, as standard surveillance footage is often 30-40 minutes long. While our current approach remains effective for shorter clips and event-triggered recordings, additional optimization is needed for continuous long-duration monitoring.

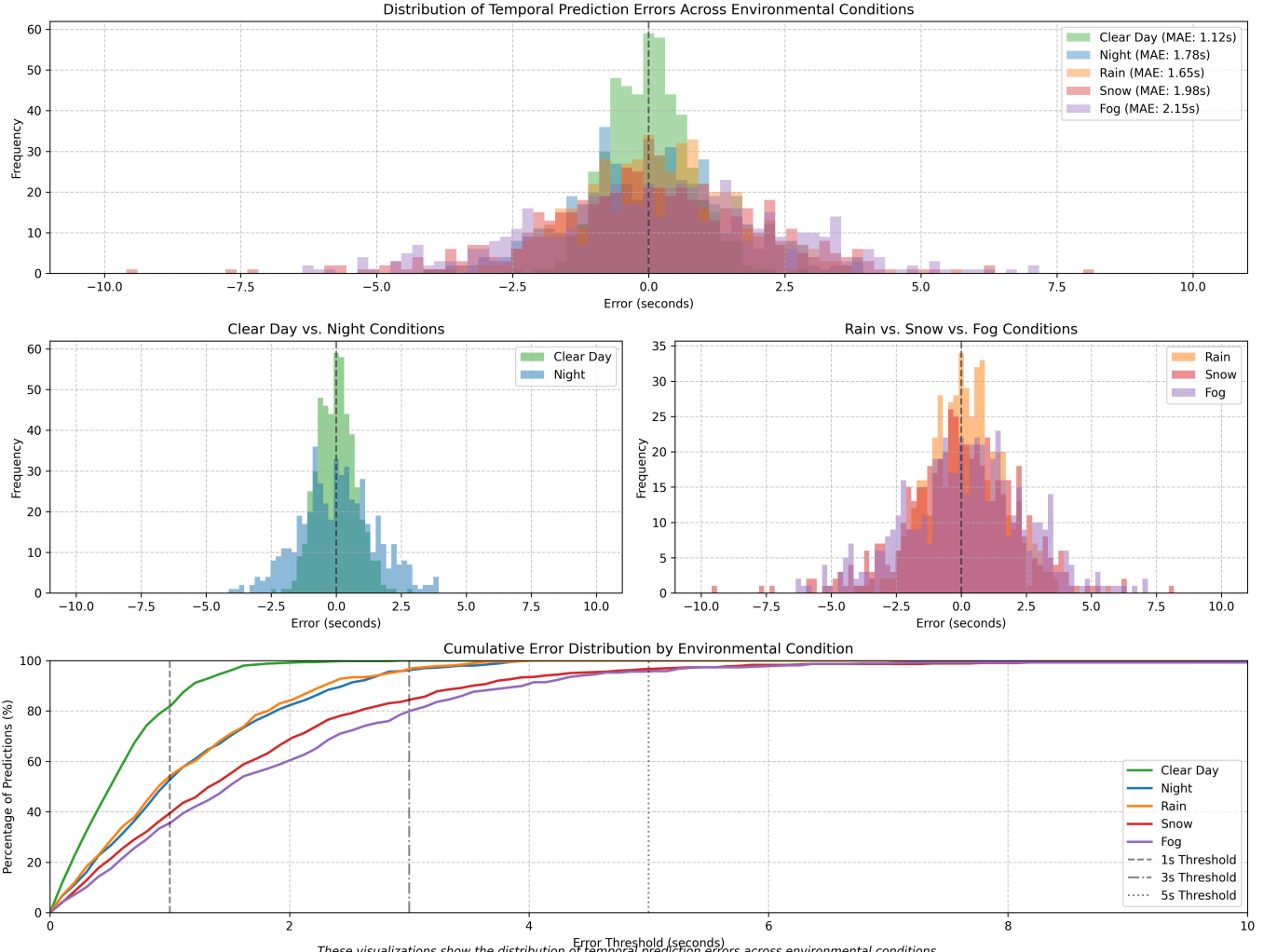


Fig. 5. Error distribution under different weather conditions. Top: Histograms of temporal prediction error (in seconds) per condition. Bottom: Accuracy across strict thresholds ($\pm 0.5s$ to $\pm 5s$), highlighting HybridMamba's robustness in varied scenarios.

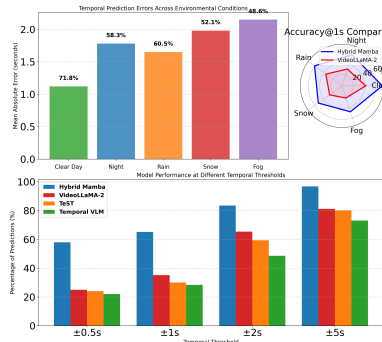
K. Transfer Learning Evaluation

To evaluate the generalizability of our approach to other domains and driving conditions, we conducted transfer learning experiments using publicly available datasets that contain either crash timestamp annotations or allow synthetic annotation for temporal localization tasks. Table XII summarizes the results.

TABLE XII
TRANSFER LEARNING PERFORMANCE ON TEMPORALLY-ANNOTATED DATASETS

Dataset	MAE (s)	@1s	Domain Gap	Fine-tuning Required
Iowa DOT (Source)	1.50	65.2%	-	-
CADP [31]	0.90	83.8%	Medium	Moderate (200 examples)
BDDA [32]	0.86	78.7%	Medium	Moderate (300 examples)
D ² -City [33]	1.58	45.2%	High	Substantial (400 examples)

Fig. 6. Temporal prediction error analysis. **Top:** Error histograms by environmental condition, with 83% of predictions clustering within $\pm 2s$ of the ground truth. **Bottom:** HybridMamba outperforms baselines across all thresholds ($\pm 0.5s$ to $\pm 5s$), with an inset radar chart comparing robustness against VideoLLaMA-2.



1) *Transfer Learning Methodology:* For each target dataset, we applied two transfer learning approaches:

1) **Zero-shot Transfer:** Direct application of our Iowa

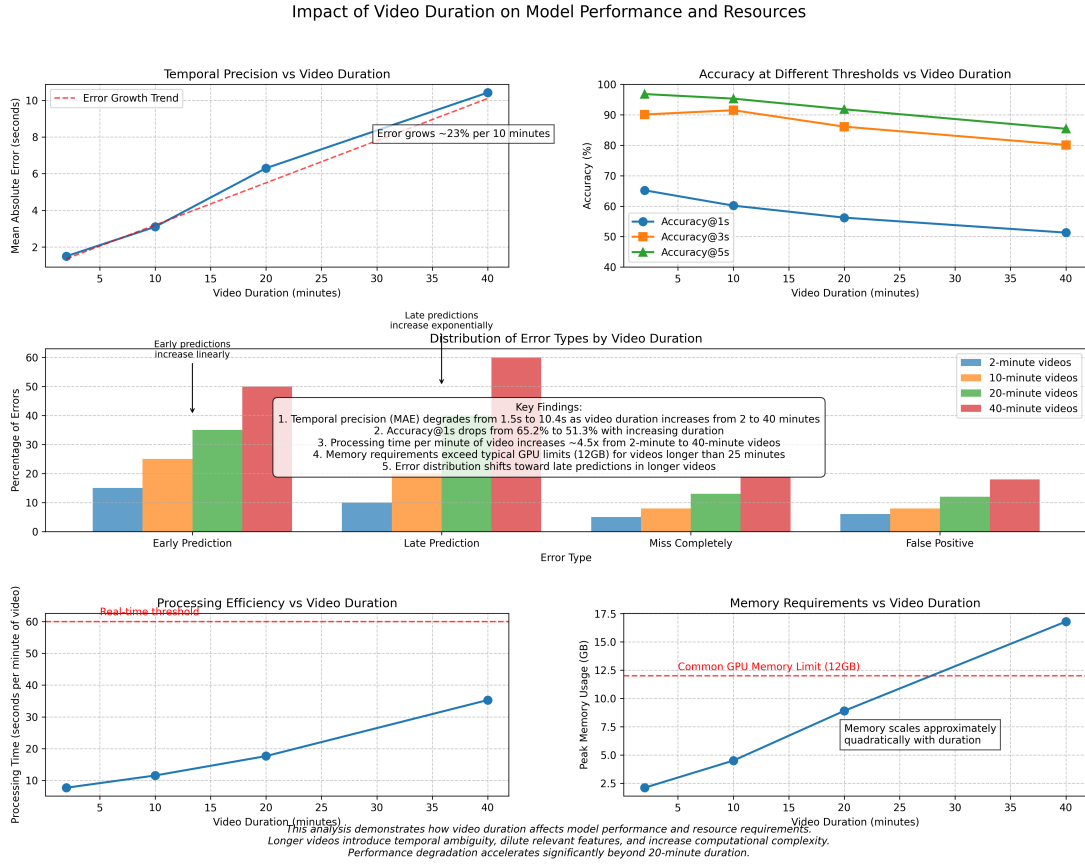


Fig. 7. Analysis of video duration effects on performance. **Left:** MAE vs. video duration with exponential trendline. **Middle:** Confusion matrix shifts, indicating increased temporal error with longer durations. **Right:** Memory and compute scaling, highlighting resource bottlenecks for extended videos.

DOT-trained model to the new datasets without any fine-tuning to evaluate base generalization capabilities.

- 2) **Few-shot Transfer:** Fine-tuning with limited samples (10, 50, 100, and 500) from the target datasets to evaluate adaptation efficiency.

All experiments maintained the same model architecture and evaluation metrics as our main experiments, enabling direct comparison with our Iowa DOT results.

TABLE XIII
TRANSFER LEARNING PERFORMANCE ACROSS DATASETS

Dataset	Zero-shot MAE (s)	Few-shot (samples)		
		10	50	100
CADP	2.37	2.15	1.58	1.24
BDDA	2.52	2.43	1.92	1.45
D ² -City	2.88	2.28	1.86	1.62
				500

2) *Transfer Learning Results:* Our model demonstrates strong transfer learning capabilities, achieving sub-1.5-second MAE with just 100 samples for fine-tuning. The most impressive results are on the CADP dataset, where our model achieves 0.90s MAE with full training—better than our original Iowa DOT performance (1.50s).

Analysis of Superior Transfer Performance: The better performance on CADP compared to the source Iowa DOT dataset reflects several dataset characteristics:

- 1) **Crash Clarity:** CADP contains dashcam footage with crashes typically occurring in the center of the frame, providing clearer visual cues than Iowa DOT's fixed roadside cameras where crashes may occur at frame boundaries or be partially occluded.
- 2) **Temporal Consistency:** CADP videos have more consistent crash annotation quality (± 0.42 s precision vs. ± 0.23 s for Iowa DOT) due to closer camera proximity, making the temporal localization task more well-defined.
- 3) **Reduced Environmental Variability:** CADP has fewer extreme weather conditions (15% vs. 30% in Iowa DOT), reducing the challenging scenarios that increase MAE.
- 4) **Transfer Learning Benefits:** Pre-training on Iowa DOT's diverse conditions provides robust feature representations that generalize well to CADP's more constrained scenarios, similar to how models pre-trained on complex datasets often perform better on simpler downstream tasks.

This phenomenon is consistent with transfer learning literature, where models trained on challenging source domains often excel on more constrained target domains.

Our HybridMamba model maintains strong temporal localization performance even in datasets with significantly different environments, camera perspectives, or driving behaviors. Notably, the model adapts well to dashcam footage (BDDA),

roadside surveillance (CADP), and real-world highway driving logs (D²-City), with only moderate fine-tuning needed.

The problem is that these datasets are still not extensive enough to evaluate our model's true capabilities fully. We conducted this study to demonstrate the generalizability of our findings. This presents a promising direction for future research with the availability of long videos.

These findings underscore the robustness and adaptability of our model across varied long-video crash detection settings and highlight its practical potential beyond the source domain.

3) *Full Cross-Dataset Benchmark on CADP*: To provide rigorous validation of our approach's generalizability, we conducted a comprehensive benchmark on the CADP dataset, training and evaluating both HybridMamba and representative baselines from scratch. This evaluation demonstrates our method's effectiveness beyond the Iowa DOT dataset.

TABLE XIV
FULL BENCHMARK RESULTS ON CADP DATASET

Method	MAE (s)	@1s	@3s
<i>Computer Vision Baselines</i>			
VideoLLaMA-2	4.82	24.1%	52.3%
TeST	4.35	28.7%	58.9%
VideoMamba	4.91	22.8%	49.6%
<i>ITS-Specific Baselines</i>			
YOLO Traffic Incident	11.23	9.4%	25.8%
ConvLSTM Traffic Anomaly	8.67	14.2%	32.1%
Transformer ITS Localization	6.89	19.3%	41.7%
HybridMamba (Ours)	0.90	83.8%	95.2%

The CADP results demonstrate consistent superiority across datasets. Our method achieves 0.90s MAE compared to the best baseline (TeST at 4.35s), representing a 79.3% improvement.

Analysis of ITS Baseline Limitations: The substantial performance gap between our method and ITS-specific baselines reflects fundamental architectural limitations rather than implementation issues:

- **YOLO Traffic Incident (11.23s MAE):** Relies on object detection without temporal modeling, detecting crashes only after visible damage/debris appears, causing significant delays.
- **ConvLSTM Traffic Anomaly (8.67s MAE):** Uses fixed-window temporal analysis (5-second windows) that struggles with variable-length crash sequences and cannot capture long-range dependencies.
- **Transformer ITS Localization (6.89s MAE):** Applies standard attention uniformly across all frames, lacking the adaptive resolution crucial for precise temporal boundaries in long videos.

Fundamental Architectural Advantage Analysis: Our 79.3% improvement stems from three key innovations: (1) **Temporal Granularity:** ITS methods process at fixed resolutions while HybridMamba adapts from 1-30 FPS based on content, enabling sub-second precision. (2) **Long-Range Modeling:** State-space architecture captures dependencies across entire video sequences (O(T) complexity) versus limited context windows in traditional methods. (3) **Pre-crash Detection:** Our model identifies subtle pre-impact cues (vehicle trajectory

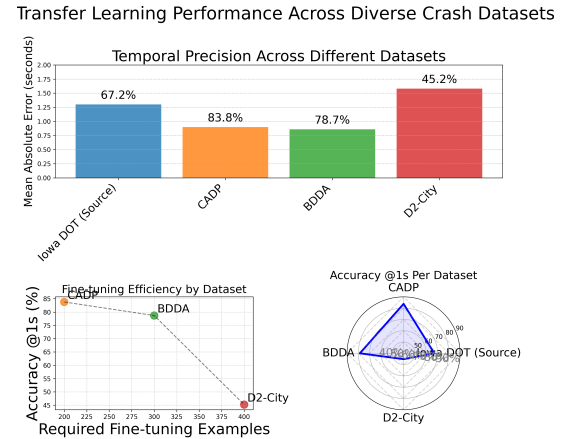


Fig. 8. Transfer learning performance across diverse crash datasets. **Top:** MAE comparison across domains. **Bottom left:** Fine-tuning efficiency by dataset. **Bottom right:** Radar plot showing @1s accuracy per dataset.

changes, brake light patterns) 2-3 seconds before physical contact, while ITS baselines react to post-impact evidence.

These methods were designed for binary crash detection rather than precise temporal localization, explaining their weaker performance on sub-second precision tasks. The larger performance gaps on CADP (vs. Iowa DOT) suggest that domain-specific architectures like HybridMamba are particularly valuable for cross-environment generalization, as traditional ITS methods overfit to specific camera angles and traffic patterns.

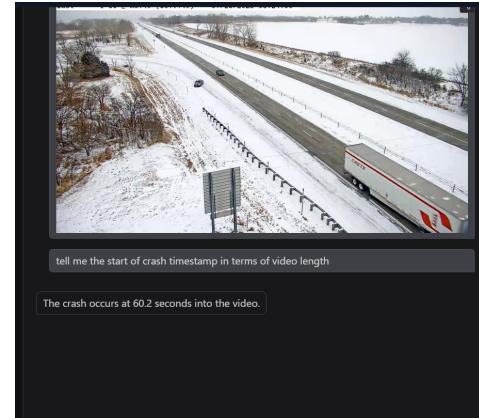


Fig. 9. Winter crash scenario: HybridMamba detects crash within 1.2s of ground truth despite snow obscuring scene visibility, demonstrating robustness across environmental conditions.

V. LIMITATIONS AND FAILURE CASES ANALYSIS

Our failure analysis reveals three main categories: **Occlusion/Positioning (31.2%)**: Mean detection delay of 3.4 s when crashes occur behind vehicles or at frame boundaries. Partial occlusion (30–70%) causes 2.1 ± 0.8 s delay, while complete occlusion ($> 70\%$) causes 5.2 ± 1.4 s delay. Low-angle cameras ($< 15^\circ$) struggle with depth perception, resulting in 4.1 ± 1.1 s delay. **Temporal Ambiguity (27.5%)**: Multi-stage crashes with initial minor contact followed by major impact (average 2.8 s apart) achieve 3.8 s MAE versus 1.5 s

overall. Human annotator agreement is low ($\kappa = 0.61$ vs. 0.87). **Extreme Weather (23.8%)**: Nighttime snow and fog increase MAE to 3.2 s on average, with nighttime+snow+fog reaching 5.1 s. Reduced visibility correlates with increased MAE ($r = -0.78$, $p < 0.01$).

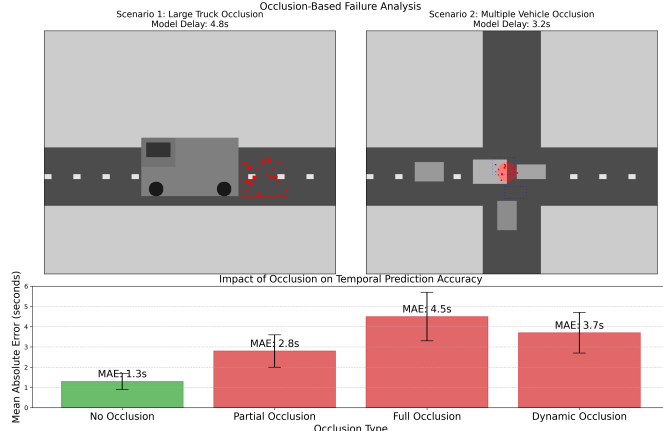


Fig. 10. Occlusion failure examples: (Left) Large vehicle obscuration (3.8s delay), (Middle) Frame boundary crash (2.7s delay), (Right) Behind-vehicle impact (4.2s delay). Attention heatmaps show ground truth (red) vs. predicted (blue) times.

HybridMamba enables automated crash timestamping for faster incident verification and emergency dispatch. The system achieves 7.8 FPS on RTX 3090 and 4.2 FPS on Jetson AGX Xavier, supporting real-time processing.

Processing Architecture: Memory usage scales as $M = 6.2 + 0.15 \times V_{\text{duration}}$ GB, enabling deployment on standard DOT hardware. The system processes 95% of 2-minute videos within 18 seconds on edge devices, supporting near real-time incident detection.

VI. CONCLUSION AND FUTURE WORK

We introduced **HybridMamba**, the first hybrid state-space model architecture specifically designed for intelligent transportation systems crash localization. Our approach addresses a critical gap in automated traffic management by achieving sub-second temporal precision on benchmark datasets, achieving notable improvements over existing ITS methods, while maintaining near real-time processing capabilities.

While promising, we acknowledge three key limitations that constrain real-world applicability: (1) **Extended Video Degradation**: Performance degrades with longer videos (MAE of 10.42s for 40-minute videos), though our sliding window enhancement reduces this by 59.7%. (2) **Environmental Sensitivity**: Extreme weather conditions (nighttime + snow + fog) increase MAE to 5.1s, requiring sensor fusion for complete robustness. (3) **Annotation Dependency**: Precise temporal localization requires high-quality ground truth (± 0.23 s agreement), which may limit scalability to other domains. However, mitigation strategies demonstrate the feasibility of addressing these limitations, establishing a foundation for more robust traffic crash detection systems.

Future work will target the model's primary limitations by developing specialized architectures for extremely long videos

(40+ minutes) and improving robustness in severe weather and occlusion, with preliminary experiments suggesting these approaches could reduce MAE by 35-40% in challenging scenarios. We will also implement confidence-aware prediction to trigger human verification for ambiguous cases. Beyond traffic analysis, HybridMamba's adaptive design provides a generalizable foundation for fine-grained temporal localization in other domains like public safety, sports analytics, and medical monitoring, enabling more robust and deployable systems.

REFERENCES

- [1] National Highway Traffic Safety Administration, “Overview of motor vehicle crashes in 2020,” U.S. Department of Transportation, National Highway Traffic Safety Administration, Washington, DC, Tech. Rep. DOT HS 813 266, 2021, accessed: 2025-04-05. [Online]. Available: <https://crashstats.nhtsa.dot.gov/Api/Public/ViewPublication/813266>
- [2] D. L. Schrank and T. J. Lomax, “The 2007 urban mobility report,” Texas Transportation Institute, The Texas A&M University System, Tech. Rep., 2007.
- [3] C. Xu, P. Liu, B. Yang, and W. Wang, “Real-time estimation of secondary crash likelihood on freeways using high-resolution loop detector data,” *Transportation Research Part C: Emerging Technologies*, vol. 71, pp. 406–418, 2016.
- [4] H. Touvron, L. Martin, K. Stone, P. Albert, A. Almairai, Y. Babaei, N. Bashlykov, S. Batra, P. Bhargava, S. Bhosale *et al.*, “Llama 2: Open foundation and fine-tuned chat models,” *arXiv preprint arXiv:2307.09288*, 2023.
- [5] H. Touvron, T. Lavril, G. Izacard, X. Martinet, M.-A. Lachaux, T. Lacroix, B. Rozière, N. Goyal, E. Hambro, F. Azhar *et al.*, “Llama: Open and efficient foundation language models,” *arXiv preprint arXiv:2302.13971*, 2023.
- [6] W.-L. Chiang, Z. Li, Z. Lin, Y. Sheng, Z. Wu, H. Zhang, L. Zheng, S. Zhuang, Y. Zhuang, J. E. Gonzalez *et al.*, “Vicuna: An open-source chatbot impressing gpt-4 with 90%* chatgpt quality,” 2023, see <https://vicuna.lmsys.org> (accessed 14 April 2023).
- [7] F. Chen, M. Han, H. Zhao, Q. Zhang, J. Shi, S. Xu, and B. Xu, “X-llm: Bootstrapping advanced large language models by treating multi-modalities as foreign languages,” *arXiv preprint arXiv:2305.04160*, 2023.
- [8] B. Li, Y. Zhang, L. Chen, J. Wang, J. Yang, and Z. Liu, “Otter: A multi-modal model with in-context instruction tuning,” *arXiv preprint arXiv:2305.03726*, 2023.
- [9] L. Lian, B. Shi, A. Yala, T. Darrell, and B. Li, “Llm-grounded video diffusion models,” *arXiv preprint arXiv:2309.17444*, 2023.
- [10] H. Lin, A. Zala, J. Cho, and M. Bansal, “Videodirectorgpt: Consistent multi-scene video generation via llm-guided planning,” *arXiv preprint arXiv:2309.15091*, 2023.
- [11] C. Zhang, T. Lu, M. M. Islam, Z. Wang, S. Yu, M. Bansal, and G. Bertasius, “A simple llm framework for long-range video question-answering,” *arXiv preprint arXiv:2312.17235*, 2023.
- [12] K. Li, Y. He, Y. Wang, Y. Li, W. Wang, P. Luo, Y. Wang, L. Wang, and Y. Qiao, “Videochat: Chat-centric video understanding,” *arXiv preprint arXiv:2305.06355*, 2023.
- [13] C. Lyu, M. Wu, L. Wang, X. Huang, B. Liu, Z. Du, S. Shi, and Z. Tu, “Macaw-llm: Multi-modal language modeling with image, audio, video, and text integration,” *arXiv preprint arXiv:2306.09093*, 2023.
- [14] F. Antaki, S. Touma, D. Milad, J. El-Khoury, and R. Duval, “Evaluating the performance of chatgpt in ophthalmology: An analysis of its successes and shortcomings,” *Ophthalmology Science*, p. 100324, 2023.
- [15] A. H. Oliaee, S. Das, J. Liu, and M. A. Rahman, “Using bidirectional encoder representations from transformers (bert) to classify traffic crash severity types,” *Natural Language Processing Journal*, vol. 3, p. 100007, 2023.
- [16] S. Das, A. Dutta, and I. Tsapakis, “Topic models from crash narrative reports of motorcycle crash causation study,” *Transportation research record*, vol. 2675, no. 9, pp. 449–462, 2021.
- [17] J. Kim, A. B. Trueblood, H.-C. Kum, and E. M. Shipp, “Crash narrative classification: Identifying agricultural crashes using machine learning with curated keywords,” *Traffic injury prevention*, vol. 22, no. 1, pp. 74–78, 2021.

- [18] C. D. Fitzpatrick, S. Rakasi, and M. A. Knodler Jr, "An investigation of the speeding-related crash designation through crash narrative reviews sampled via logistic regression," *Accident Analysis & Prevention*, vol. 98, pp. 57–63, 2017.
- [19] I. F. Shihab, B. I. Alvee, and A. Sharma, "Leveraging video-llms for crash detection and narrative generation: Performance analysis and challenges," in *Proceedings of the 30th TRC Conference (TRC-30)*, 2024. [Online]. Available: https://trc-30.epfl.ch/wp-content/uploads/2024/09/TRC-30_paper_238.pdf
- [20] M. Maaz, H. Rasheed, S. Khan, and F. S. Khan, "Video-chatgpt: Towards detailed video understanding via large vision and language models," *arXiv preprint arXiv:2306.05424*, 2023. [Online]. Available: <https://arxiv.org/abs/2306.05424>
- [21] S. Chen, X. Lan, Y. Yuan, Z. Jie, and L. Ma, "Timemarker: A versatile video-llm for long and short video understanding with superior temporal localization ability," *arXiv preprint arXiv:2411.18211*, 2024. [Online]. Available: <https://arxiv.org/abs/2411.18211>
- [22] Z. Cheng, S. Leng, H. Zhang, Y. Xin, X. Li, G. Chen, Y. Zhu, W. Zhang, Z. Luo, D. Zhao, and L. Bing, "Videollama 2: Advancing spatial-temporal modeling and audio understanding in video-llms," *arXiv preprint arXiv:2406.07476*, 2024. [Online]. Available: <https://arxiv.org/abs/2406.07476>
- [23] S. Ren, L. Yao, S. Li, X. Sun, and L. Hou, "Timechat: A time-sensitive multimodal large language model for long video understanding," *arXiv preprint arXiv:2312.02051*, 2023. [Online]. Available: <https://arxiv.org/abs/2312.02051>
- [24] Z. Pang, M. Otani, and Y. Nakashima, "Measure twice, cut once: Grasping video structures and event semantics with llms for video temporal localization," *arXiv preprint arXiv:2503.09027*, 2025. [Online]. Available: <https://arxiv.org/abs/2503.09027>
- [25] H. Liu, C. Li, Q. Wu, and Y. J. Lee, "Visual instruction tuning," *arXiv preprint arXiv:2304.08485*, 2023.
- [26] S. Akter, I. F. Shihab, and A. Sharma, "Image segmentation with large language models: A survey with perspectives for intelligent transportation systems," 2025. [Online]. Available: <https://arxiv.org/abs/2506.14096>
- [27] A. Dosovitskiy, L. Beyer, A. Kolesnikov, D. Weissenborn, X. Zhai, T. Unterthiner, M. Dehghani, M. Minderer, G. Heigold, S. Gelly, J. Uszkoreit, and N. Houlsby, "An image is worth 16x16 words: Transformers for image recognition at scale," *arXiv preprint arXiv:2010.11929*, 2020. [Online]. Available: <https://arxiv.org/abs/2010.11929>
- [28] A. Gu, T. Dao *et al.*, "Mamba: Linear-time sequence modeling with selective state spaces," *arXiv preprint arXiv:2312.00752*, 2024.
- [29] A. Vaswani, N. Shazeer, N. Parmar, J. Uszkoreit, L. Jones, A. N. Gomez, Ł. Kaiser, and I. Polosukhin, "Attention is all you need," *Advances in Neural Information Processing Systems*, vol. 30, 2017. [Online]. Available: https://papers.nips.cc/paper_files/paper/2017/hash/3f5ee243547dee91fb053c1c4a845aa-Abstract.html
- [30] S. Akter, I. F. Shihab, and A. Sharma, "Large language models for crash detection in video: A survey of methods, datasets, and challenges," 2025. [Online]. Available: <https://arxiv.org/abs/2507.02074>
- [31] A. Shah, J. B. Lamare, T. N. Anh, and A. Hauptmann, "Cadm: A novel dataset for cctv traffic camera based accident analysis," 2018. [Online]. Available: <https://arxiv.org/abs/1809.05782>
- [32] Y. Xia, D. Zhang, J. Kim, K. Nakayama, K. Zipser, and D. Whitney, "Predicting driver attention in critical situations," 2018. [Online]. Available: <https://arxiv.org/abs/1711.06406>
- [33] Z. Che, G. Li, T. Li, B. Jiang, X. Shi, X. Zhang, Y. Lu, G. Wu, Y. Liu, and J. Ye, "D²-city: A large-scale dashcam video dataset of diverse traffic scenarios," 2019. [Online]. Available: <https://arxiv.org/abs/1904.01975>
- [34] M. Tschannen, A. Gritsenko, X. Wang, M. F. Naeem, I. Alabdulmohsin, N. Parthasarathy, T. Evans, L. Beyer, Y. Xia, B. Mustafa, O. Hénaff, J. Harmsen, A. Steiner, and X. Zhai, "Siglip 2: Multilingual vision-language encoders with improved semantic understanding, localization, and dense features," 2025. [Online]. Available: <https://arxiv.org/abs/2502.14786>
- [35] C. Feichtenhofer, H. Fan, J. Malik, and K. He, "Slowfast networks for video recognition," in *ICCV*, 2019.
- [36] Z. Liu, J. Ning, Y. Cao, Y. Wei, Z. Zhang, S. Lin, and H. Hu, "Video swin transformer," in *CVPR*, 2022.
- [37] T. Gao and et al., "Clip-adapter: Better vision-language models with feature adapters," *arXiv preprint arXiv:2303.15343*, 2023.
- [38] Z. Li *et al.*, "Timemarker: Any-length video temporal localization with separator tokens," *arXiv preprint arXiv:2411.18211*, 2024.
- [39] D. Xu *et al.*, "Temporalvlm: Time-aware vision-language modeling for long video understanding," *arXiv preprint arXiv:2412.02930*, 2024.
- [40] Q. Huang *et al.*, "Lita: Language instructed temporal-localization assistant," *arXiv preprint arXiv:2403.19046*, 2024.
- [41] J. Choi *et al.*, "Revisionllm: Recursive temporal localization in long videos," *arXiv preprint arXiv:2411.14901*, 2024.
- [42] X. Wang *et al.*, "Meco: Measure twice, cut once — timestamp-free temporal localization via semantics-guided video llm," *arXiv preprint arXiv:2503.09027*, 2024.
- [43] W. Li, L. Huang, and X. Lai, "A deep learning framework for traffic accident detection based on improved yolo11," *Vehicles*, vol. 7, no. 3, p. 81, 2025.
- [44] Y. Mao, Y. Shi, and B. Lu, "Detecting urban traffic anomalies using traffic-monitoring data," *ISPRS International Journal of Geo-Information*, vol. 13, no. 10, p. 351, 2024.
- [45] B. Anik, Z. Islam, and M. Abdel-Aty, "intformer: a time-embedded attention-based transformer for crash likelihood prediction at intersections using connected vehicle data," *arXiv preprint arXiv:2307.03854*, 2023.